

## Electrocatalytic properties of $\gamma$ -NiOOH nanolayers, synthesized by successive ionic layer deposition, during the oxygen evolution reaction upon water splitting in the alkaline medium

A. A. Lobinsky, V. P. Tolstoy, I. A. Kodinzev

Institute of Chemistry, Saint Petersburg State University,  
26 University Pr., St. Peterhof, Saint Petersburg, 198504, Russia

lobinsky.a@gmail.com, v.tolstoy@spbu.ru, i.a.kod@mail.ru

PACS 82.65+r

DOI 10.17586/2220-8054-2018-9-5-669-675

Nickel oxyhydroxide nanolayers were synthesized on the surface of nickel foam and single crystalline silicon through Successive Ionic Layer Deposition (SILD) method by using aqueous solutions  $\text{NiSO}_4$  and  $\text{K}_2\text{S}_2\text{O}_8$ . The obtained nanolayers were characterized by SEM, XRD, FTIR and XPS spectroscopy. The electrochemical properties of the electrodes were defined from polarization curves. SEM images revealed that nanolayers are formed by nanosheets with a thickness of 6 – 10 nm. The nanolayers were shown to exhibit electrocatalytic properties during the oxygen evolution reaction upon water splitting in the alkaline medium. By setting the number of SILD cycles, these properties can be changed precisely. For a number of samples, synthesized after 30 – 120 SILD cycles, it was found that in the oxygen evolution reaction the lowest overpotential value of 260 mV and the lowest Tafel slope of 54 mV/dec are achieved for the sample, synthesized after 90 SILD cycles.

**Keywords:** NiOOH, nanolayers, SILD, oxygen evolution reaction.

*Received: 21 August 2018*

### 1. Introduction

One of the practical approaches to hydrogen production is the splitting of water. Recently it has grown in importance due to the development of new methods for energy conservation, including renewable ones. The method of energy conservation during electrolytic water splitting allows working the problems of cyclicality and instability of energy receiving in solar and wind power areas as well as those of free capacity use during periods of no peak hours, for instance, in the nuclear power field. One of the significant features of the energy conversion is its environmental friendliness, since this process only requires water and electricity. Today it is important to reduce energy consumption for water electrolysis in such devices through overpotential reduction on the electrodes which is caused by using specific electrocatalysts. Even having been developing for more than 40 years, the history of these electrocatalysts has recently gained interest due to production of new electrocatalysts, composed of generally available transition metals such as Ni, Co and Fe [1–3]. It was mentioned [4] that catalysts based on nickel oxides or hydroxides, exhibiting high stability to oxidation in alkaline medium, are among the best.

Taking into account the practical importance of challenges to synthesize electrocatalysts, to date, a variety of methods of preparative inorganic chemistry has been used. The methods had been previously tested by producing a wide range of other metal-oxygen compounds. Such methods include, for example, sol-gel [5], hydrothermal [6], coprecipitation [7], electrochemical [8] etc.

Meanwhile, analysis of the literature reveals that there are few works describing Layer-by-Layer (LbL) synthesis as method to obtain such electrocatalysts. These include, for example, the works, devoted to the synthesis of electrocatalytic layers  $\text{IrO}_2$  [9] and  $\text{Co}_3\text{O}_4$  [10]. This method of synthesis based on a successive and multiple treatments of substrate in salt or colloidal solutions and polyelectrolytes, forming an insoluble nanolayers of new compound upon interaction at the surface. The SILD method is one of LbL synthesis methods without the using of polyelectrolyte solutions. We believe there are particular advantages in using SILD synthesis to create highly efficient electrocatalysts: the possibility to deposit nanolayers with a precisely defined thickness onto the surface of the electrodes of complex shape, producing such nanolayers under "soft chemistry" conditions almost at room temperature, the use of diluted and available metal salts solutions in synthesis, etc. These features of the SILD synthesis had defined its efficiency, for example, when creating new supercapacitor electrodes [11], superparamagnetic materials [12], sensors active elements [13], etc.

The purpose of this work is to study the electrocatalytic properties of  $\gamma$ -NiOOH nanolayers, synthesized by SILD method using the previously proposed synthesis scheme with salts  $\text{NiSO}_4$  and  $\text{K}_2\text{S}_2\text{O}_8$  [14], for the oxygen evolution reaction upon water splitting in the alkaline KOH solution.

## 2. Experimental methods

Nickel foam plates by AO (JSC) "ECAT" with a porosity of 80 PPI and a size of approximately  $5 \times 25$  mm, pressed to 0.25 mm, as well as plates of single crystalline silicon with orientation of  $\langle 100 \rangle$  and a size of approximately  $0.35 \times 10 \times 25$  mm were used as substrates for synthesis of nanolayers. Before the synthesis, nickel foam substrates had been treated according to the method [15], namely in acetone using ultrasonication for 30 minutes and then in 6 M HCl solution for 15 minutes to remove the oxide layer. Further, the substrates were washed with deionized water three times and air-dried at  $70^\circ\text{C}$  for 30 minutes. Single crystalline silicon wafers were washed in acetone to remove the organic impurities and etched in concentrated HF for 15 minutes, then washed in distilled water multiple times to remove the acid excess. After that they were treated for 20 minutes in the diluted KOH solution with  $\text{pH} \sim 9,0$ .

The synthesis of nanolayers was conducted using SILD method, utilizing  $\text{NiSO}_4$  solution as the precursor with a concentration of 0.01 M and the equilibrium pH value as well as  $\text{K}_2\text{S}_2\text{O}_8$  solution with a concentration of 0.01 M and  $\text{pH} = 10.5$ , achieved by adding 0.5 M aq. KOH to the  $\text{K}_2\text{S}_2\text{O}_8$  solution dropwise. During the synthesis, the substrates were fixed in a holder of a special automated setup and successively immersed for 30 seconds in chemical vessels with  $\text{NiSO}_4$  solution, distilled water,  $\text{K}_2\text{S}_2\text{O}_8$  solution and distilled water again. Such treatment constituted one SILD cycle, which has been repeated several times.

XRD patterns were obtained using a Rigaku Miniflex II X-ray diffractometer with  $\text{Cu } K\alpha$  radiation ( $\lambda = 0.154056$  nm). The morphology and composition of synthesized films was investigated by SEM at accelerating voltage 4 kV on Zeiss Merlin microscope and EDX used detector Oxford INCAx-act. FTIR transmission spectra of synthesized films on silicon surface were registered by FCM-2201 spectrophotometer using differential technique with respect to spectra of bare silicon plate. X-ray photoelectron spectroscopy (XPS) was obtained used ESCALAB 250Xi electron spectrometer, with  $\text{Al } K\alpha$  radiation (14.866 eV).

Electrocatalytic characteristics of electrodes for oxygen evolution reaction were recorded using potentiostat Elins P-45X and a three-electrode cell, where an electrode based on the pressed nickel foam with an electroactive substance, deposited via SILD method, and electroactive area of  $0.5 \text{ cm}^2$  was used as a working one. The  $\text{Ag}/\text{AgCl}$  electrode and a platinum foil were used as reference electrode and counter electrode, respectively. Overpotentials, recorded in this study, were calibrated for a reversible hydrogen electrode ( $E_{RHE}$ ) according to the Nernst equation  $E_{RHE} = E_{\text{Ag}/\text{AgCl}}^0 + 0.059 \cdot \text{pH} + E_{\text{Ag}/\text{AgCl}}$ , where  $E_{\text{Ag}/\text{AgCl}}^0$  is a standard potential for the  $\text{Ag}/\text{AgCl}$  electrode (0.197 mV), and  $E_{\text{Ag}/\text{AgCl}}$  is the potential for the  $\text{Ag}/\text{AgCl}$  electrode, obtained in the measurement. All the measurements have been carried out at room temperature and atmospheric pressure in 1 M aq. KOH ( $\text{pH} = 14$ ) solution as electrolyte. Polarization curves were usually shot at scan rate of 5 mV/sec. Overpotential ( $\eta$ ) was determined from the polarization curve, obtained through linear potential sweep with IR compensation, as the difference between the recorded potential (at a current density of  $10 \text{ mA}/\text{cm}^2$ ) and water splitting potential for the reversible hydrogen electrode of 1.23 V.

## 3. Results

As shown in the electron micrograph (Fig. 1), in the composition of the nanolayers, synthesized after 50 SILD cycles, it is possible to separate individual flat nanocrystals approximately 6 – 10 nm thick, oriented mainly perpendicular to the surface of the substrate. We assume that the appearance of such mainly oriented nanocrystals on the surface is a proof of the previously established model of their growth [16], which is based on the idea of the formation of the 2D  $\text{NiOOH}$  nanocrystals arranged in the same plane on the surface after the first SILD cycles. These nanocrystals possess the morphology of nanosheets that, as the number of SILD cycles increases, change their planar geometry due to the repulsive interaction of areas of equal charge. These equally charged nanosheets appear on the surface in each SILD cycle at the stages of treatment in salt solutions, when the adsorption of, for instance, cations  $\text{Ni}^{2+}$  appears on the surface.

Figure 2 shows an X-ray diffraction pattern, where the peaks at  $22.4$ ,  $44.6$ ,  $50.3^\circ$  are to be noted, and which, according to JCPDS 06-0075, can be attributed to the crystal planes (003), (102) and (105) of  $\gamma$ - $\text{NiOOH}$  with hexagonal crystal structure; as well as peaks at  $22.4$ ,  $40.1$ ,  $43.3$ ,  $72.4$  and  $78.5^\circ$  that, according to JCPDS 06-0144, are related to  $\text{Ni}_3\text{O}_2(\text{OH})_4$  planes (003), (100), (006), (110) and (114) and have the hexagonal structure too. It can be noticed that in the latter compound some of the Ni cations have the oxidation state of 2+. Unfortunately, it is impossible to determine the percentage of each compound from the X-ray diffraction pattern because of the width of the observed peaks, which is related to the nanosize of such crystals. However, we can state that the synthesis results in the formation of  $\gamma$ - $\text{NiOOH}$  nanocrystals on the substrate surface. After being in air for several days these nanocrystals partly transform in  $\text{Ni}_3\text{O}_2(\text{OH})_4$  nanocrystals. This effect can be noted visually by observing that the color of the as-prepared synthesized samples changes and becomes lighter after drying and storage on air. At the

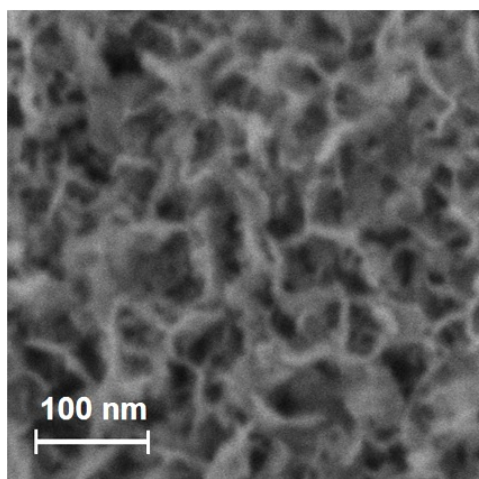


FIG. 1. The SEM micrograph of the nanolayer synthesized after 50 SILD cycles

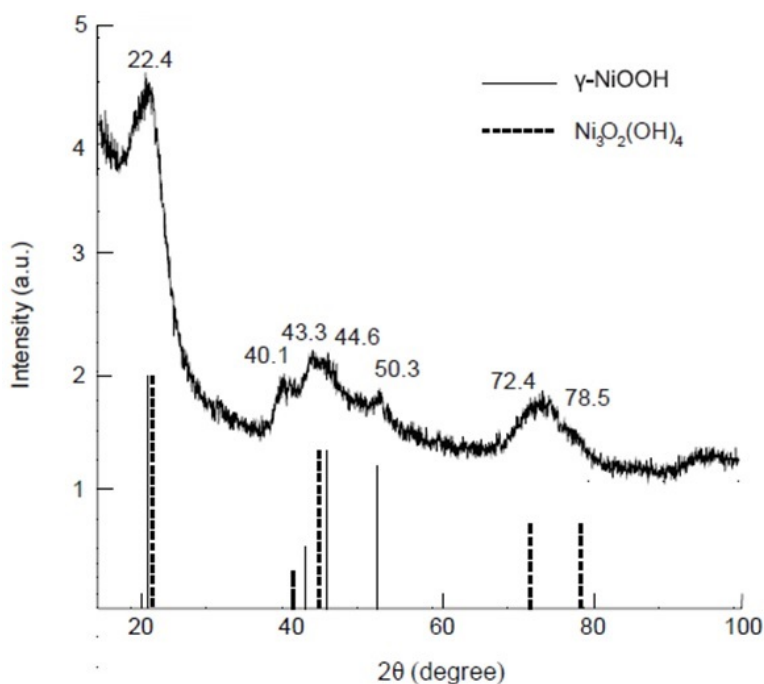


FIG. 2. X-ray diffraction pattern of the nanolayer synthesized after 50 SILD cycles

same time, we cannot exclude the incomplete oxidation of  $\text{Ni}^{2+}$  cations during the sample treatment in  $\text{K}_2\text{S}_2\text{O}_8$  solution because the reaction proceeds in alkaline medium, where, in the first place, the hydrolysis of cations is to be seen and only after that - their oxidation. We assume that the bi-phase composition of the investigated nanolayers has no effect on the electrocatalytic properties of such nanolayers because in the OER the nanolayers of the electrocatalyst is on the anode's surface, and under electrolysis conditions the positive voltage is applied on that nanolayers. The voltage is higher than the oxidation potential  $\text{Ni}^{2+} \rightarrow \text{Ni}^{3+}$ , due to which all  $\text{Ni}^{2+}$  ions become  $\text{Ni}^{3+}$  ions and it is  $\gamma$ -NiOOH that is involved in the electrocatalysis.

The study of the nanolayers by FTIR spectroscopy revealed a spectrum, shown in Fig. 3. The spectrum happens to be similar to the spectrum, recorded in [14]. As can be seen from the Fig. 3, the composition of the nanolayers includes water molecules, corresponding to absorption bands with peaks at  $3440\text{ cm}^{-1}$  and  $1640\text{ cm}^{-1}$ . According to [17], bands with peaks at  $1470$  and  $1383\text{ cm}^{-1}$  can be attributed to carbon-oxygen stretching vibrations in  $\text{CO}_3^{2-}$  anions, which apparently appeared on the surface due to the adsorption of  $\text{CO}_2$  molecules upon sample contact with the atmosphere. We can also mention an adsorption band with peak at  $1083\text{ cm}^{-1}$ ,

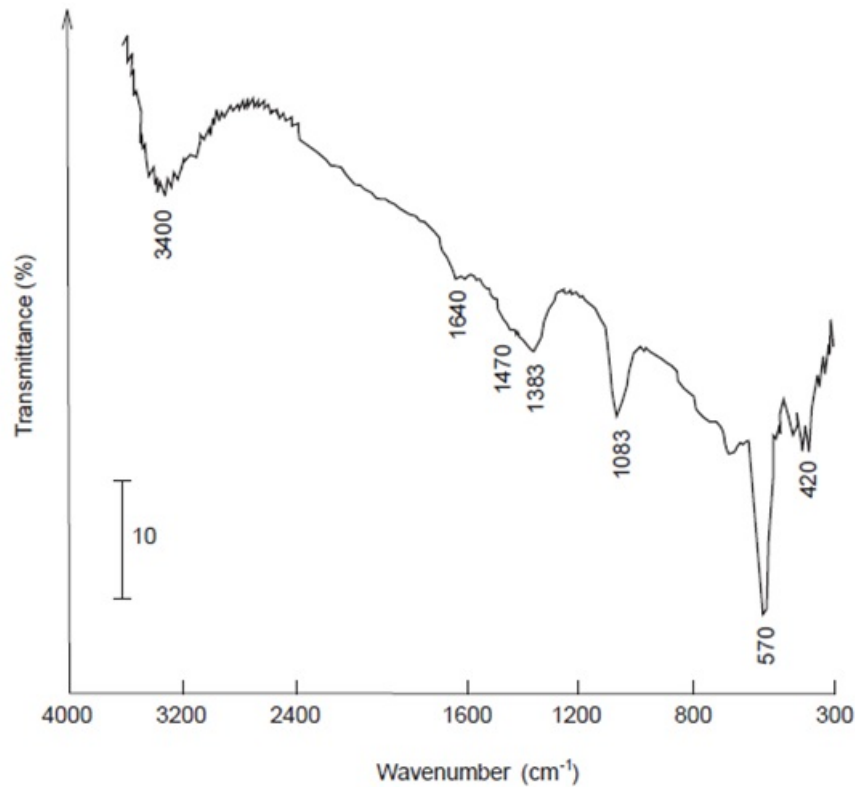


FIG. 3. FTIR transmittance spectrum of nanolayer synthesized on the silicon surface after 50 SILD cycles

corresponding to S-O stretching vibrations in sulfate anions [17], remained apparently in the nanolayers after the synthesis that involved the above mentioned reagent solutions. A band with peak at  $570\text{ cm}^{-1}$  can be attributed to  $\text{Ni}^{3+}$ -O stretching vibrations in  $\gamma\text{-NiOOH}$ , and a band with peak at  $420\text{ cm}^{-1}$  – to  $\text{Ni}^{2+}$ -O stretching vibrations in  $\text{Ni}_3\text{O}_2(\text{OH})_4$  [18–20].

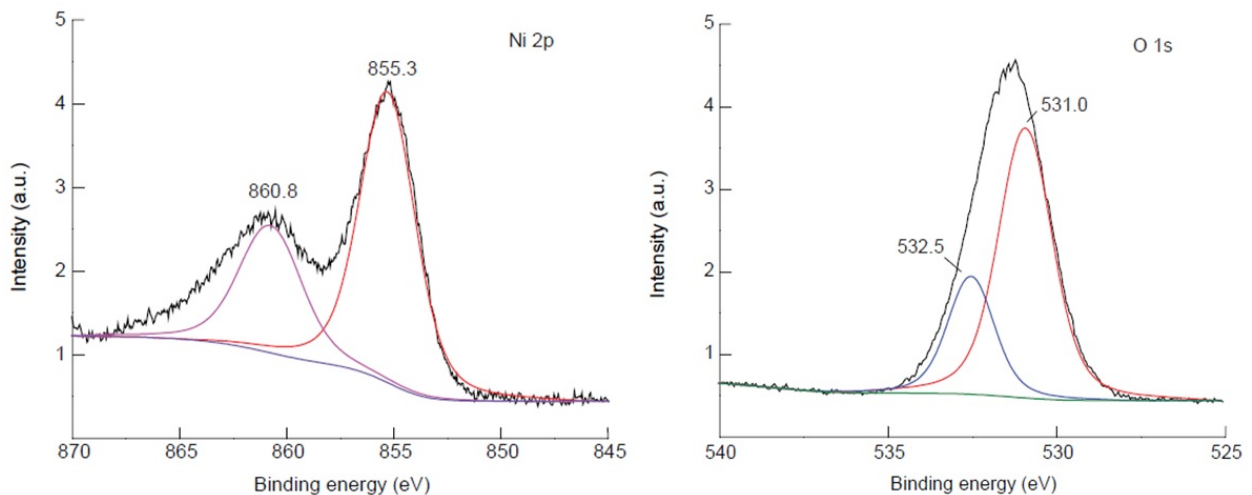


FIG. 4. X-ray photoelectron spectra of Ni 2p and O 1s electrons of the nanolayer, synthesized on the silicon surface after 50 SILD cycles

Figure 4 shows X-ray photoelectron spectra in the energy range typical for Ni 2p and O 1s electrons. Broad peaks at 855.3 eV and 860.8 eV can be attributed, similar to work [21], to the signals from Ni  $2p_{3/2}$  and  $2p_{1/2}$  electrons in the oxidation states of 3+ and 2+. The peaks at 531.0 eV and 532.5 eV can be attributed to the signals

from 1s electrons of O atoms in Ni-OH and to those from adsorbed H<sub>2</sub>O, respectively [22]. When analysing XPS results, indicating the presence of Ni of two oxidation states in the nanolayers, it should be taken into account that Ni<sup>3+</sup> hydroperoxides are partly unstable after being kept in air for several days, as noted in [23].

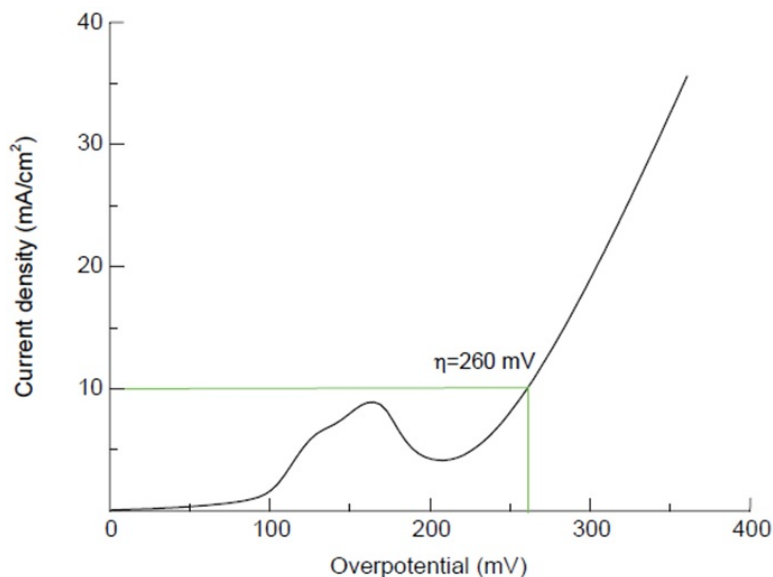


FIG. 5. LSV curve of the nickel foam electrode with nanolayer synthesized after 90 SILD cycles

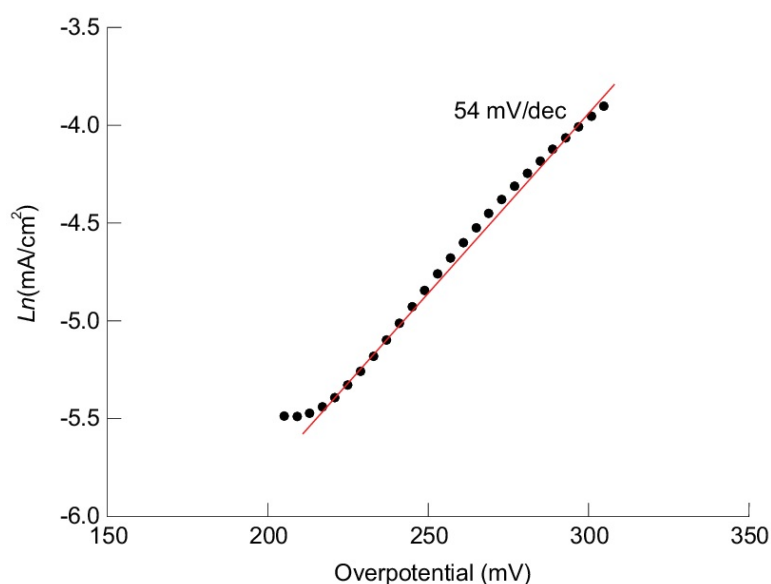


FIG. 6. Tafel plot of the nickel foam electrode with nanolayer synthesized after 90 SILD cycles

As an example of the results obtained experimentally from the studying of electrocatalytic properties of obtain nanolayers. Fig. 5. shows the change of current density vs. overpotential for the electrode based on nickel foam and nanolayer, synthesized after 90 SILD cycles. From the figure can be observed that overpotential value at a current density of 10 mA/cm<sup>2</sup> is 260 mV. An important parameter characterising the microkinetics of catalytic processes in OER is the Tafel slope, which can be measured as the current density logarithm versus overpotential. The calculation of Tafel slope for this sample from the data obtained allowed finding its value, which was 54 mV/dec (Fig. 6).

The analysis of overpotential and Tafel slope values has been carried out for a series of electrocatalysts samples synthesized after various number of SILD cycles. The results of the analysis are presented in Table 1. The table

shows that as the number of SILD cycles increases, overpotential and Tafel slope values decrease, however after 120 SILD cycles they increase insignificantly. That allowed us to choose an electrocatalyst nanolayer, synthesized after 90 SILD cycles, as the one with the optimal properties. This effect of the properties' change in a series of similar samples, synthesized after various number of SILD cycles, is apparently due to the fact that as the number of SILD cycles increases, the number of nanocrystals of the catalytically active species on the surface of nickel foam increases as well. However, after 90 treatment cycles the nanolayers have relatively high electrical resistivity, which leads to the increase of overpotential and Tafel slope values.

In general, it should be mentioned that the obtained results are close, and in some cases even superior, to the electrocatalytic characteristics of similar materials, synthesized by other methods [24–26]. We can assume that this is due to the unique morphological features of the obtained  $\gamma$ -NiOOH nanocrystals and to the presence of pores between them that contribute to the more effective removal of oxygen bubbles in that electrochemical process. The similar assumption has been made in the work [27] that studied electrocatalytic properties of Ni/Sn layers. An important feature of the proposed synthesis method of the electrocatalytic material is the possibility to set the conditions of the synthesis precisely. For instance, by setting the number of SILD cycles and therefore by obtaining a series of similar samples of electrocatalysts, among which we can choose the samples with optimal electrochemical characteristics. Undoubtedly, the properties of such materials can be further improved, particularly, by doping the nanolayers with various electrocatalytically active metals. However, this subject is beyond the scope of this article.

TABLE 1. A comparison of overpotential and Tafel slope values for nickel foam-based electrodes and nickel oxyhydroxides nanolayers synthesized after different number of SILD cycles

Number of SILD	Overpotential, mV at current density 10 mA/cm <sup>2</sup>	Tafel slope, mV/dec
30	305	63
60	293	60
90	260	54
120	278	56

#### 4. Conclusion

The treatment of nickel foam according to SILD method by NiSO<sub>4</sub> and K<sub>2</sub>S<sub>2</sub>O<sub>8</sub> solutions with the equilibrium pH value and pH = 10.5, respectively, allows synthesis a nanolayers of nickel oxyhydroxides on the surface of nickel foam. The nanolayers contains  $\gamma$ -NiOOH and Ni<sub>3</sub>O<sub>2</sub>(OH)<sub>4</sub> nanocrystals with nanosheet morphology, the sheets are 6 – 10 nm thick and are oriented mainly perpendicular to the substrate surface. The nanolayers shows electrocatalytic properties during the oxygen evolution reaction upon water splitting in the alkaline medium, which can be changed precisely by setting synthesis conditions, namely, the number of SILD cycles. For a number of samples, synthesized after 30 – 120 SILD cycles, it was found experimentally that in the oxygen evolution reaction the minimum overpotential value of 260 mV and the minimum value of Tafel slope of 54 mV/dec are achieved for the sample, synthesized after 90 SILD cycles.

#### Acknowledgement

This work was supported by the Russian Science Foundation (project No. 18-19-00370). We grateful to the Centres for X-ray Diffraction Studies, Nanotechnology and Physical Methods of Surface Investigation of Saint-Petersburg State University for their technical assistance with the investigation of the synthesized product.

#### References

- [1] Bandal H., Koteswara Reddy K., Chaugule A., Kim H. Iron-based heterogeneous catalysts for oxygen evolution reaction; change in perspective from activity promoter to active catalyst. *J. Power Sources*, 2018, **395**, P. 106–127.
- [2] Hunter B.M., Winkler J.R., Gray H.B. Iron is the active site in nickel/iron water oxidation electrocatalysts. *Molecules*, 2018, **4**, P. 903–910.
- [3] Ya Yan, Bao Yu Xia, Bin Zhao, Xin Wang. A review on noble-metal-free bifunctional heterogeneous catalysts for overall electrochemical water splitting. *J. Mater. Chem. A*, 2016, **4**, P. 17587–17603.
- [4] Yuanyuan Ma, Xiaoli Dong, Renhe Wang, Duan Bin, Yonggang Wang, Yongyao Xia. Combining water reduction and liquid fuel oxidation by nickel hydroxide for flexible hydrogen production. *Energy Storage Materials*, 2018, **11**, P. 260–266.
- [5] Sarycheva A.S., Semenova A.A., Goodilin E.A. Vapor phase SERS sensor based on mesoporous silica decorated with silver nanoparticles. *Nanosystems: Physics, Chemistry, Mathematics*, 2017, **8**(5), P. 579–585.

- [6] Krasilin A.A., Gusarov V.V. Redistribution of Mg and Ni cations in crystal lattice of conical nanotube with chrysotile structure. *Nanosystems: Physics, Chemistry, Mathematics*, 2017, **8**(5), P. 620–627.
- [7] Nguyen A.T., Phan Ph.H.Nh., Mittova I.Ya., Knurova M.V., Mittova V.O. The characterization of nanosized ZnFe<sub>2</sub>O<sub>4</sub> material prepared by coprecipitation. *Nanosystems: Physics, Chemistry, Mathematics*, 2016, **7**(3), P. 459–463.
- [8] Mingshu Xiao, Yanping Tian, Yuhua Yan, Kai Feng, Yuqing Miao. Electrodeposition of Ni(OH)<sub>2</sub>/NiOOH in the presence of urea for the improved oxygen evolution. *Electrochimica Acta*, 2015, **164**, P. 196–202.
- [9] Hidalgo-Acosta J.C., Scanlon M.D., Méndez M.A., Amstutz V., Vrube H., Opallo M., Giraulta H.H.. Boosting water oxidation layer-by-layer. *Phys. Chem. Chem. Phys.*, 2016, **13**, P. 9295–9304.
- [10] Bryan H.R. Suryanto, Xunyu Lua, Chuan Zhao. Layer-by-layer assembly of transparent amorphous Co<sub>3</sub>O<sub>4</sub> nanoparticles/graphene composite electrodes for sustained oxygen evolution reaction. *J. Mater. Chem. A*, 2013, **1**, P. 12726–12731.
- [11] Lobinsky A.A., Tolstoy V.P. Red-ox reactions in aqueous solutions of Co(OAc)<sub>2</sub> and K<sub>2</sub>S<sub>2</sub>O<sub>8</sub> and synthesis of CoOOH nanolayers by the SILD method. *Nanosystems: Physics, Chemistry, Mathematics*, 2015, **6**(6), P. 1–7.
- [12] Kuklo L.L., Tolstoy V.P. Successive ionic layer deposition of Fe<sub>3</sub>O<sub>4</sub>@HxMoO<sub>4</sub>·nH<sub>2</sub>O composite nanolayers and their superparamagnetic properties. *Nanosystems: Physics, Chemistry, Mathematics*, 2016, **7**(6), P. 1050–1054.
- [13] Tolstoy V.P., Kodintsev I.A., Reshanova K.S., Lobinsky A.A. A brief review of metal oxide (hydroxide)-graphene nanocomposites synthesis by layer-by-layer deposition from solutions and synthesis of CuO nanorods-graphene nanocomposite. *Rev. Adv. Mater. Sci.*, 2017, **49**, P. 28–37.
- [14] Lobinsky A.A., Tolstoy V.P., Gulina L.B. A novel oxidation-reduction route for successive ionic layer deposition of NiO<sub>1+x</sub>·nH<sub>2</sub>O nanolayers and their capacitive performance. *Materials Research Bulletin*, 2016, **76**, P. 229–234.
- [15] Mingjun Pang, Guohui Long, Shang Jianc, Yuan Ji, Wei Han, Biao Wang, Xilong Liu, Yunlong Xi. One pot low-temperature growth of hierarchical d-MnO<sub>2</sub> nanosheets on nickel foam for supercapacitor applications. *Electrochim. Act.*, 2015, **161**, P. 297–304.
- [16] Lobinsky A.A., Tolstoy V.P., Gulina L.B. Direct synthesis of Co<sub>2</sub>Al(OH)<sub>7–2x</sub>(CO<sub>3</sub>)<sub>x</sub>·nH<sub>2</sub>O layered doublehydroxide nanolayers by successive ionic layer deposition and their capacitive performance. *Applied Surface Science*, 2014, **320**, P. 609–613.
- [17] Tolstoy V.P., Chernyshova I.V., Skryshevsky V.A. *Handbook of infrared spectroscopy of ultrathin films*. John Wiley & Sons, Inc., Hoboken, New Jersey, 2003, 710 p.
- [18] Kashani M.M., Youzbashi A.A., Hashemzadeh F., Sabaghzadeh L. Structural properties of nickel hydroxide/oxyhydroxide and oxide nanoparticles obtained by microwave-assisted oxidation technique. *Powder Technol.*, 2013, **237**, P. 562–568.
- [19] Cerc Korošeca R., Bukoveca P., Pihlar B., Šurca Vukb A., Orelb B., Dražič G. Preparation and structural investigations of electrochromic nanosized NiO<sub>x</sub> films made via the sol-gel route. *Solid State Ionics*, 2003, **165**, P. 191–200.
- [20] Ren Y., Chim W.K., Guo L., Tanoto H., Pan J., Chiam S.Y. The coloration and degradation mechanisms of electrochromic nickel oxide. *Solar Energy Mater. Solar Cells*, 2013, **116**, P. 83–88.
- [21] Gui Chen, Lingjing Chen, Siu-Mui Ng, Tai-Chu Lau. Efficient chemical and visible-light-driven water oxidation using nickel complexes and salts as precatalysts. *Chem. Sus. Chem.*, 2014, **7**, P. 127–134.
- [22] Biesinger M.C., Payne B.P., Grosvenor A.P., Lau L.W.M., Gerson A.R., Smart R.St.C. Resolving surface chemical states in XPS analysis of first row transition metals, oxides and hydroxides: Cr, Mn, Fe, Co and Ni. *Appl. Surf. Sci.*, 2011, **257**, P. 2717–2730.
- [23] Fomanyuk S.S. Electrochromic and gasochromic properties thin films of nickel hydroxide. *Metal physics and advanced technologies*, 2011, **33**, P. 297–306.
- [24] Kim B., Oh A., Kabiraz M.K., Hong Y., Joo J., Baik H., Choi S.-I., Lee K. NiOOH exfoliation-free nickel octahedra as highly active and durable electrocatalysts toward the oxygen evolution reaction in an alkaline electrolyte. *ACS Appl. Mater. Interfaces*, 2018, **10**, P. 10115–10122.
- [25] Qiong Zhang, Cancan Zhang, Jianbo Liang, Penggang Yin, Yang Tian. Orthorhombic  $\alpha$ -NiOOH nanosheet arrays: phase conversion and efficient bifunctional electrocatalysts for full water splitting. *ACS Sustainable Chem. Eng.*, 2017, **5**(5), P. 3808–3818.
- [26] Diaz-Morales O., Ferrus-Suspedra D., Koper M.T.M. The importance of nickel oxyhydroxide deprotonation on its activity towards electrochemical water oxidation. *Chem Sci.*, 2016, **7**(4), P. 2639–2645.
- [27] Cian-Tong Lu, Yen-Wen Chiu, Mei-Jing Li, Kan-Lin Hsueh, Ju-Shei Hung. Reduction of the electrode overpotential of the oxygen evolution reaction by electrode surface modification. *Int. J. of Electrochem.*, 2017, **2017**, 7494571.